

QUT Digital Repository:
<http://eprints.qut.edu.au/>



This is the published version of this journal article:

Doherty, William O.S. and Rackemann, Darryn W. and Steindl, Roderick J. (2010) *Fouling of tubular ceramic membranes during processing of cane sugar juice*. *Desalination and Water Treatment*, 16. pp. 45-56.

© Copyright 2010 the authors.



Fouling of tubular ceramic membranes during processing of cane sugar juice

W. O. S. Doherty*, D. W. Rackemann, R. J. Steindl

Sugar Research and Innovation, Centre for Tropical Crops and Biocommodities, Queensland University of Technology, 2 George Street, Brisbane, 4001, Australia
Tel. +61 (7) 3138 1655; Fax +61 (7) 3138 4132; email: w.doherty@qut.edu.au, d.rackemann@qut.edu.au

Received 5 March 2009; Accepted 23 November 2009

ABSTRACT

This paper examines the fouling characteristics of four tubular ceramic membranes with pore sizes 300 kDa, 0.1 μm and 0.45 μm installed in a pilot plant at a sugar factory for processing clarified cane sugar juices. All the membranes, except the one with a pore size of 0.45 μm , generally gave reproducible results through the trials, were easy to clean and could handle operation at high volumetric concentration factors.

Analysis of fouled and cleaned ceramic membranes revealed that polysaccharides, lipids and to a lesser extent, polyphenols, as well as other colloidal particles cause fouling of the membranes. Electrostatic and hydrophobic forces cause strong aggregation of the polymeric components with one another and with colloidal particles. To combat irreversible fouling of the membranes, treatment options that result in the removal of particles having a size range of 0.2–0.5 μm and in addition remove polymeric impurities, need to be identified.

Chemical and microscopic evaluations of the juices and the structural characterisation of individual particles and aggregates identified options to mitigate the fouling of membranes. These include conditioning the feed prior to membrane filtration to break up the network structure formed between the polymers and particles in the feed and the use of surfactants to prevent the aggregation of polymers and particles.

Keywords: Ceramic membranes; Fouling; Membrane filtration; Sugar juice

1. Introduction

Juice clarification is critical unit process in the raw sugar factory. The aims of the clarification process are to remove suspended and colloidal particles, remove non-sugar soluble impurities (e.g. proteins, polysaccharides and inorganic materials) and raise the juice pH to minimise inversion of sucrose during subsequent processing. The effectiveness of the clarification process affects the juice filterability, evaporator efficiency, sucrose crystallisation and the quality and quantity of raw sugar produced. Poor clarification can impact

negatively on the colour, crystal morphology, crystal content, ash and polysaccharide content of raw sugar. Membrane filtration is typically used as an additional processing step to improve the clarified juice quality by removing large amounts of polysaccharides, turbidity and colloidal impurities. The removal of these impurities has a significant impact on the viscosity of subsequent processing streams and allows significant processing efficiency gains and improved sugar quality to be achieved [1,2].

Early research that evaluated the possibilities of using membrane processes to concentrate and purify sugar cane juices [3] reported that ultrafiltration of sugar cane could not compete economically with conventional

*Corresponding author.

filtration processes at 30°C due to fouling problems. Since this early work [1], commercial organizations manufacturing and/or supplying membrane systems to the sugar industry became actively involved in the installation and development of pilot plants into sugar factories [4–11]. Several sugar factories and milling companies have also assessed the benefits of membrane filtration systems to their factories either independently or in conjunction with membrane suppliers [2,12].

Despite the extensive investigations, the only full scale industrial installation of membrane technology in the cane sugar industry occurred at Puunene factory, Maui, Hawaii [13]. The installation operated from late 1994 until late 1998 when it was shut down as a result of many factors including maintenance and operational costs. A smaller scale membrane installation has been employed as part of the white sugar milling (WSM) technology at one South African factory as an alternative process to produce white sugar at the sugar. The WSM plant processes a small fraction (~15%) of the total factory juice [14]. Other workers [15,16] reported that irreversible fouling of the membranes leading to reduced flux also contributed to slow adoption of the technology by sugar factories.

In order to quantify the benefits of membrane filtration for the Australian sugar industry, a comprehensive research investigation using a pilot plant supplied by Applexion was undertaken in an Australian sugar factory. Tubular ceramic membranes composed of a hard porous baked alumina/titania support on which is bonded zirconium oxide to affect membrane pore size/selectivity were examined. A range of operating conditions were used and the data obtained were then used to develop a model to predict the permeate flux levels under different operating conditions which is being published elsewhere. This paper presents only the results on the foulants (including those that cause irreversible fouling) obtained with the tubular ceramic membranes used in the Applexion pilot plant when processing clarified juices.

2. Materials and methods—pilot plant

The pilot plant supplied by Applexion was fully equipped with instrumentation and controllers. The schematic of the Applexion pilot plant is shown in Fig. 1 and the plant contains (a) pre filters, (b) feed and recirculation pumps (c) feed buffer tank, (d) two modules for the ceramic membranes (e) heat exchanger with thermostatically controlled valve and a number of magnetic flow meters, pressure gauges and temperature sensors. The filter areas for the membranes investigated is given in Table 1 and end views of the two types of ceramic membranes are shown in Fig. 2.

The trials were conducted over two crushing seasons, using clarified juice feed at temperatures between 80 and 98°C; volumetric concentration factors (VCF) between 2 and 10× and feed velocities between 3.9 and 5.1 m.s⁻¹. The Applexion pilot plant operated by varying the transverse membrane pressure (TMP) to maintain a relatively constant VCF and permeate flux. The retentate flow was adjusted using a pressure valve to control the VCF. In the first hour the TMP was ramped from 0.1 to 1 bar to provide a steadily imposed load to minimise stress on the equipment. Subsequently the VCF was maintained by increasing the TMP (to a pre-determined limit of 4 bar) to maintain the permeate rate as the membranes foul.

2.1. Juice and membrane analyses

Major factors involved in solute separation by membranes are (a) intrinsic rejection by the membrane of a specific solute, and (b) the nature of the concentration polarization layer at the surface of the porous filtration medium. Interactions of juice components during membrane filtration result in complex modifications of the impurities at the membrane surface [17]. Based on this information, it was necessary that studies on the physico-chemical properties of both the fouled and cleaned membrane, and the filtered and unfiltered clarified juices be carried out.

Juice samples from the feed, permeate and retentate streams obtained from operation with the membranes were stored frozen prior to analysis.

2.2. Membrane analysis

Sections of cleaned and fouled KB-W-07 ceramic membranes (see Fig. 3) labeled (a) and (b) respectively were stored at -4°C for further analysis. The 'cleaned' membrane was cleaned in place (CIP) (during the factory trials) using the CIP recommendation of Applexion. The nearness to pre-trial water flux measurements was used as an indication of the effectiveness of the cleaning procedure based on measuring the flux while processing clean water and correlating this value to a reference condition of 25°C and 4 bar.

Cleaning was recommended to be undertaken when the maximum TMP was reached and the flux started to decline. The CIP involved four sequential chemical cycles including:

- 0.034 L of 50% NaOH per 1 m³.h⁻¹ of clarified juice capacity;
- 0.135 L of 15% NaOCl per 1 m³.h⁻¹ of clarified juice capacity;
- 1% v/v nitric acid; and
- 0.225 L liquid detergent (Applexion supplied) per 1 m³.h⁻¹ of clarified juice capacity.

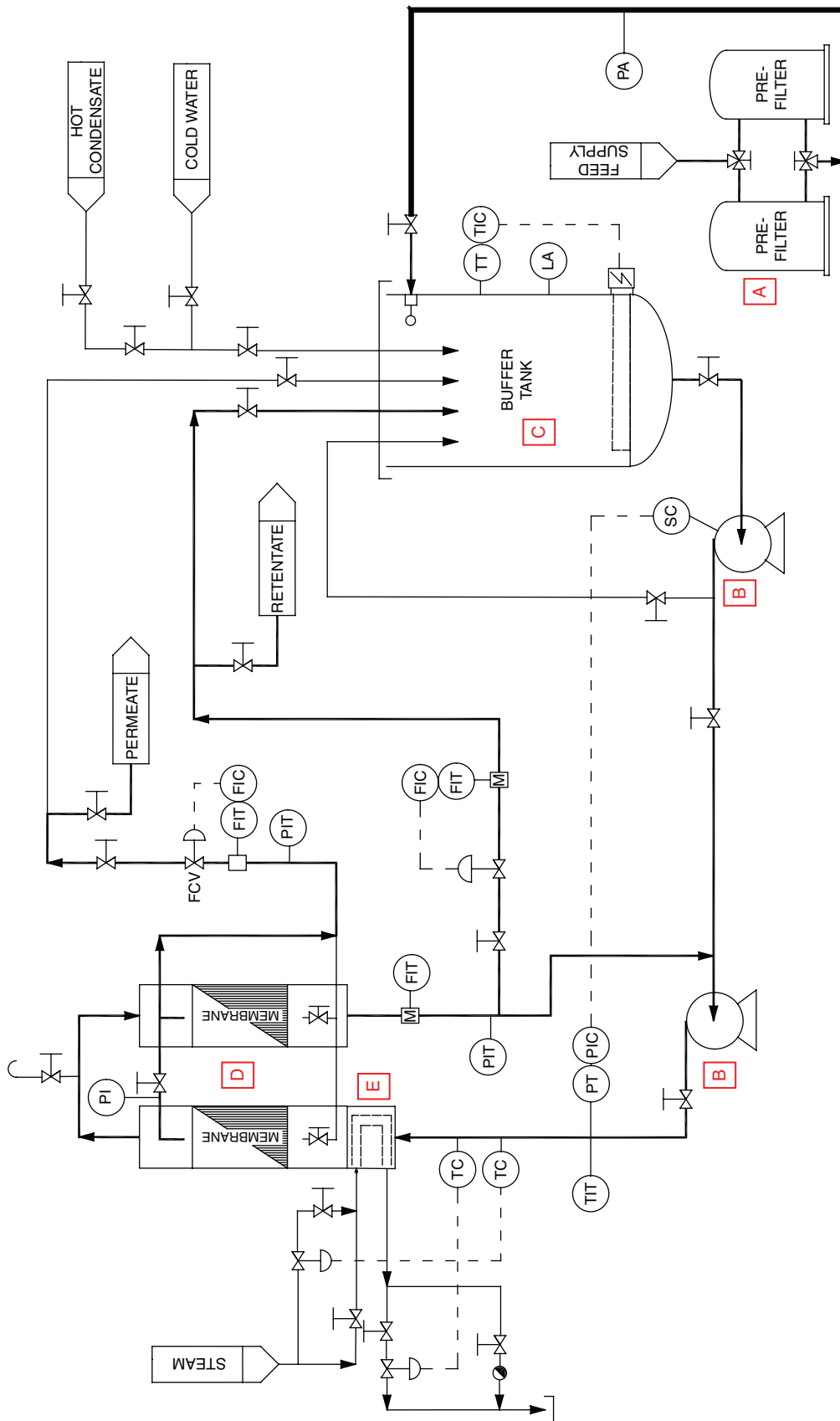


Fig. 1. Schematic of pilot plant (A – pre filters; B – feed and recirculation pumps; C – feed buffer tank; D – ceramic membrane modules; E – heat exchanger).

Table 1
Information on some of the ceramic membranes trialled.

Reference code	Membrane format	MWCO* or pore size	Flow channel diameter, mm	Total surface area, m ²
KB-W-07 (300)	Ceramic	300 kDa	3.5	3.44
KB-W-07 (01)	Ceramic	0.1 µm	3.5	3.44
KB-W-07 (045)	Ceramic	0.45 µm	3.5	3.44
KB-T	Ceramic	0.1 µm	2.6	4.90

*Molecular weight cut off.

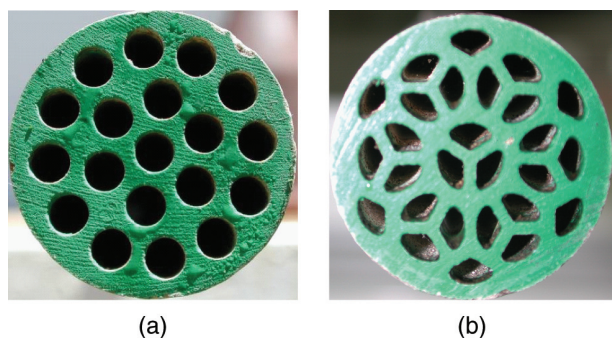


Fig. 2. End view of the (a) KB-W-07 (01) membrane and (b) KB-T membrane (N.B. membranes shown have a diameter of 25.4 mm).

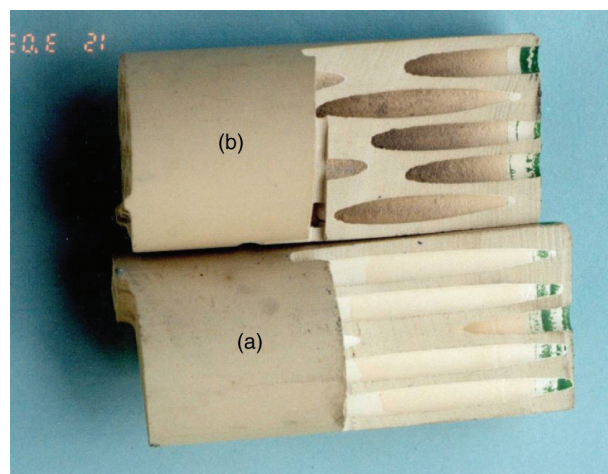


Fig. 3. Cleaned (a) and fouled (b) ceramic elements.

The clarified juice capacity of the ceramic membranes was dependent on the pore size and flow channel behaviour of the membranes and ranged between 200 and 350 L.m⁻².h⁻¹. Initial CIP trials highlighted the importance of flushing and rinsing the membranes between cleaning cycles and indicated that high quality and hot temperature water improved the overall efficiency of the cleaning process. The hottest clean water available (~85°C) was used to flush the chemicals and rinse the membranes.

Typically there are two phases of cleaning [18]. In the first stage the cleaning chemicals are mixed and adhere to the foulants and adequate time is needed for this to occur. The second stage dislodges and removes the foulants from the system. High shear (velocity for hydrodynamic forces) reduces cleaning time due to faster mixing and greater force to dislodge foulants from surfaces. Low shear rates (velocity) also mean foulants can reattach to surfaces for small periods of time and may not be completely removed from the membrane system. The detergent cleaning cycle (and rinsing steps) follow the second phase of cleaning and were found to produce the most significant flux recovery.

The Ian Wark Research Institute at the University of South Australia (IWRI) analysed membrane samples to characterise the materials adsorbed on the membrane

using X-ray photoelectron spectroscopy (XPS), time of flight secondary ion mass spectroscopy (ToF-SIMS) and diffuse reflectance infrared Fourier transform (DRIFT). These techniques give highly complementary surface speciation information. For characterisation of the samples by DRIFT, adsorbed materials were physically removed and extracts from ethanol, acetone and hexane were filtered and air-dried prior to analysis.

Membrane sections were carbon coated to a depth of ~0.5 nm. A Cam Scan scanning electron microscopy (SEM) instrument (Cambridge Instruments) using a field emission gun was used in the secondary electron mode for analysis. Imaging provided a high resolution topographical image of the different membrane sections (bulk, coat, and surface). Representative sample areas were chosen for imaging and scale bars were used to provide particle size reference points. Energy dispersive analysis of X-rays (EDAX) generated by electron interaction with the elements comprising the material surface provided additional elemental surface information.

The clean and fouled membranes were reduced to a coarse aggregate and the membrane foulants extracted

with water by Soxhlet extraction to enable proton nuclear magnetic resonance ($^1\text{H-NMR}$) spectroscopic analyses on these materials using a Bruker AM 300 spectrometer operating at 300 MHz. A proportion of each fraction was filtered through a Whatman No. 91 paper to remove particles of the ceramic membranes. The extracts were freeze dried to remove water. The membrane was Soxhlet extracted a second time using methanol to remove less hydrophilic foulants. The methanol was then removed using a rotary evaporator and the extract freeze-dried to remove residual water.

2.3. Juice analysis

Juice analyses were also conducted by the IWRI using EDAX (Cam Scan scanning electron microscope, Cambridge Instruments) to identify the elements present on a 2 μm Millipore filter after filtration of the juice samples.

Flow and oscillation rheological measurements of the juice samples were taken at 20°C with a Rheometrics SR-5000 controlled stress rheometer fitted with coaxial cylinder coquette geometry. Shear viscosity (η) measurements were made over the range 0.1–10³ s⁻¹. Dynamic mechanical measurements of the storage modulus (G') and loss modulus (G'') were made over the frequency range 0.1–10 Hz.

The surface electrical properties of the particles present in juice were determined by using an AcoustoSizer (developed jointly by the University of Sydney, Colloidal Dynamics, and Matec Applied Sciences) with measurements made over a range of frequencies between 300 kHz and 11 MHz. The particle size distribution of solid material in sugar solutions was measured by laser diffraction using a Malvern Mastersizer X. Measurements were conducted wet using a standard sample dispersion unit and water as solvent.

3. Results and discussion—flux data

The conditions of the tests conducted with each of the membrane elements are listed in Table 2. All the membranes, except the one with a pore size of 0.45 μm , generally gave reproducible results through the season, were easy to clean and could handle operation at high VCFs (up to 50 \times). The 0.45 μm membranes experienced fouling and cleaning problems that resulted in a much lower flux being obtained than expected. It is speculated that the largest pore size allowed the trapping of the largest amount of particles which completely blocked the pores. This resulted in poor cleaning since there was insufficient contact between the particles and the cleaning agents.

The important performance indicator in ultrafiltration is the volume flow rate of liquid through the membrane per unit area of membrane filter. This is defined in terms

Table 2

Details of some of the clarified juice trials using ceramic membranes.

Membrane	Temperature (°C)	VCF	Velocity (m s ⁻¹)	Initial flux (L m ⁻² h ⁻¹)	
KB-W-07 (300)	98	2	5.1	319	
	98	2	5.1	294	
	98	5	5.1	268	
	98	5.1	5	229	
	98	5	5.1	220	
	98	10.2	5.1	213	
	98	10.2	5.1	188	
	98	10.2	5.1	167	
	KB-W-07 (01) 1999 trials	86	2	5	205
90		2	5	173	
87		2	5	202	
92		2	5	252	
97		2	5	268	
83		3	5	161	
86		3	5	168	
97		3	5	215	
94		3	5	255	
95		3	5	211	
80		10	5	104	
86		10	5	127	
95		10	5	195	
KB-W-07 (01) 2000 trials	96	10	5	168	
	95	10	5	182	
	98	2	5.1	316	
	98	2.9	5.1	283	
	98	5.1	5.1	279	
	98	5	5.1	234	
	98	5	4.1	212	
	KB-W-07 (045)	97	2	5	166
		98	2.1	5	219
		98	2	5.1	149
98		5	5.1	216	
98		5.1	5.1	125	
KB-T	98	10.2	5.1	93	
	98	2.0	4.1	224	
	97	2.0	4.1	237	
	98	5.0	5.1	249	
	98	5.1	5.1	237	
	99	5.1	3.9	184	
	98	5.6	4.8	261	
	98	5.1	4.1	179	
	96	6.6	4.0	167	
	98	10.2	4.1	144	
98	10.4	4.8	207		

of the permeate flux and is expressed in units of L.m⁻².h⁻¹. Flux is dependent on a number of factors [19] including:

- Permeability of the flow through the membrane which is dependent on operating conditions (pressure) and feed characteristics such as temperature and viscosity;

- Resistance to flow by the concentration polarisation layer and fouling impurities that can accumulate in the voids (pores) of the membrane material. The concentration of these impurities will also lead to higher viscosity of the recirculating liquid; and
- Diffusivity of the flow which is affected by the turbulence and velocity (determined by the recirculating flow rate) through the membrane.

As the membranes are configured for cross-flow, the velocity and turbulence of the feed flow are important parameters that can retard the fouling mechanisms on the surface of the membrane by also assisting the scouring nature of the flow across the pores. The KBT membrane with the unique flow channel not only allowed increased surface area (increased throughput) but the flow channel profile (see Fig. 2) was designed to increase the turbulence of the flow.

The flux results in Table 2 confirm the filtration theories that show higher fluxes are obtained with low VCF, higher temperature feed (lower viscosity) higher feed velocity and higher turbulence as shown by the KB-T membranes when compared to the KB-W-07 (01) membranes (same pore size). The 0.1 μm pore size membranes also produced slightly higher fluxes compared to the 300 kDa pore size membranes.

4. Results and discussion

4.1. Characterisation of cleaned and fouled membranes

4.1.1. SEM analysis

SEM images of the fouled and cleaned membranes are shown in Fig. 4 (a) and (b). Fig. 4a shows three layers of differing topographical features as (i) the bulk ceramic body of the membrane, (ii) a surface coating (or layer) on the body of the membrane and (iii) a surface layer of the foulant species of $\sim 2 \mu\text{m}$ in thickness. This layer was absent in the cleaned membrane (Fig. 4b).

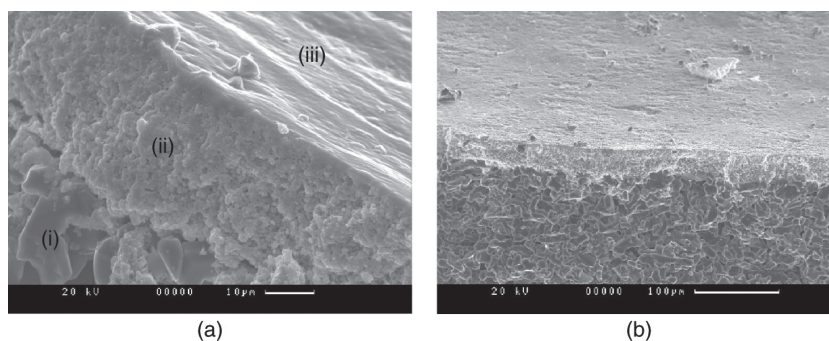


Fig. 4. SEM micrographs of (a) fouled and (b) cleaned membranes.

The SEM micrographs of the fouled membrane surface indicated regions of homogeneous layers and regions that contain particulates and holes. The individual particles on the surface were of different sizes, morphology and aspect ratios.

The EDAX spectrum of the fouled membrane indicated the presence of Al, Mg, Cl, Ca, Na and P. Calcium, Na, Cl and P were absent in the EDAX spectrum of the cleaned Na membrane. The elements Zr, Al and Ti originate from the materials used in making the ceramic membranes.

4.1.2. XPS analysis

XPS analysis was used to quantify the concentrations of the elements on the surface. It was also used to complement the EDAX data. The concentrations of the elements for both the cleaned and fouled membranes are given in Table 3. The result for the fouled membrane shows an increase in C atomic concentration and a decrease of Ti, Al and Zr compared to the clean membrane due to the presence of organic compounds. The fouled layer also contains Ca and P that originates from the feed stream. It also contains significant amounts of N which is probably associated with proteins. These results indicate that the fouled layer consists of organic (including proteins) and inorganic materials (including possibly a calcium phosphate salt).

4.1.3. ToF-SIMS analysis

The total positive and negative ions ToF-SIMS spectra of the membrane foulants were recorded from the surface of the bulk membrane. From the positive mass spectrum of the fouled membrane, the largest signals correspond to organic fragment ions CH_3^+ , C_2H^+ , C_2H_2^+ , C_2H_3^+ , C_3H_3^+ , C_3H_5^+ and C_4H_7^+ at m/z 15.02, 24.96, 25.97, 27.02, 41.04, 39.02 and 55.05 Da. Calcium is also present in minor amounts (m/z 39.96). Other peaks obtained at higher masses (e.g. 281, 342, 358 and 481 Da) correspond to polymeric species.

Table 3
Average percentage of atomic concentrations of cleaned and fouled membrane (KB-W-07 (01)) by XPS.*

Element	Cleaned	Fouled	**Fouled
C	20.6	31.6	31.5
O	69.6	58.3	57.9
Ca	0.0	0.8	0.8
Al	1.9	1.4	1.4
Zr	3.0	0.6	0.6
Na	0.0	0.7	0.7
N	0.0	3.7	3.7
Ti	4.9	2.3	2.3
Cl	0.0	0.67	0.7
P	0.0	0.0	0.6

*Average value of five readings on a surface. The error in the analysis $\pm 5\%$.

**Normalised with respect to phosphorus in the spectrum analysis.

4.1.4. DRIFT analysis

DRIFT provided functional group analysis of the fouled membrane and indicated absorption at 3165, 2870, 2845, 1629, 1521 and 827 cm^{-1} as shown in Fig. 5. The broad absorption in the 3165 cm^{-1} region corresponds to $-\text{OH}$ stretching, with associated hydrogen bonding. The strong absorption in the 2800–2900 cm^{-1} corresponded to C-H stretching and represents organic matter. Stretching from $-\text{CH}_2$ and $-\text{CH}_3$ are contained within the CH envelope. The peaks at 1521 and 827 cm^{-1} could not be assigned.

4.1.5. NMR analysis of membrane foulants

To obtain further information on the composition of the polymeric materials identified in earlier investigations, proton nuclear magnetic resonance (H-NMR) spectroscopic analyses of the foulants materials were

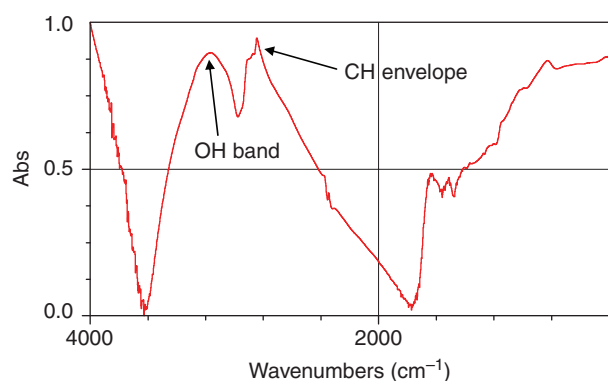


Fig. 5. DRIFT spectra of the surface foulants.

undertaken. Table 4 shows the chemical shift values for the materials extracted from the membrane with water. Also given in Table 4 are the chemical shift values for the filtered water extracts. The extracts were filtered to ensure removal of particulate matter that may interfere with the results. The H-NMR data for the material extracted from the fouled membrane with methanol are also given in Table 4. The chemical shifts of the anomeric protons in the region 5.3–5.9 ppm are indicative of α -D-linked polysaccharides e.g., dextran). In addition to polysaccharide peaks, all the samples contain aliphatic lipid signals. Table 4 also shows that the fouled membrane contains more peaks (e.g., at 6.22, 4.47, 3.41, 2.91 and 0.59 ppm) and so more compounds than the cleaned membranes. The chemical shifts at 8.74, 7.85 and 7.4 ppm found in the methanol extract are associated with phenolic aromatic rings and benzylic substituted carbonyl.

In summary, the NMR and other spectroscopic results clearly show that the foulant layer contains polysaccharides, lipids, polyphenols and nitrogenous material, probably proteins and amino acids in confirmation with previous studies [15,16]. In addition, the foulant contains Al, Mg, Cl, Ca, Na and P present in the colloidal particles. Based on the NMR, data it is concluded that the foulants that attach to the surface of the membrane are readily removed during cleaning but those that are probably trapped in the pores are more difficult to remove. It is these trapped materials that are probably responsible for the irreversible fouling of the membrane.

4.1.6. Summary

The results indicated clear differences in the chemistry and structure of the fouled and cleaned membranes. Characterization using SEM was able to differentiate a top coating (or layer) of the foulant species that was $\sim 2 \mu\text{m}$ in thickness. The top coating was mainly organic with regions of inorganic colloidal materials. This top coating was absent in the cleaned membrane.

XPS, ToF-SIMS and DRIFT analysis provided the following information:

- The fouled membrane contains polymeric species with molecular weight >400 Da.
- The foulant is rich in carbon signifying the presence of organic matter.
- The foulant is also rich in nitrogen (which is probably associated with proteins and amino acids). In addition, the foulant contains Al, Mg, Cl, Ca, Na and P.
- Proportions of the foulant can be selectively removed by fractionation.

The NMR results clearly showed that the polymeric materials consist of polysaccharides, lipids and

Table 4
Proton nuclear magnetic resonance chemical shifts (ppm) of impurities isolated from membranes.

Sample	Functional groups						
	Phenolic; benzylic sub. carbonyl	Olefinic, polar	Anomeric region polysaccharide	Ring proton region polysaccharide	Hydroxylated methylene polysaccharide	Aliphatic hydrocarbon polysaccharide	Aliphatic hydrocarbon lipids
Cleaned membrane (filtered solution)			5.87 (double peak) 5.86 5.81	4.1 (multiple peaks)	3.88		1.73 1.37
Cleaned membrane (not filtered)			5.92 5.87 (double peak) 5.86	4.1 (multiple peaks)	3.88		1.73 1.33
Fouled membrane (filtered solution)		6.22	5.73 5.63 5.51 5.31	4.16 (multiple peaks)	3.97 3.41	2.91 2.61 2.50	1.74 (multiple peaks)
Fouled membrane (not filtered)		6.23	5.92 5.68 5.50 5.30	4.74 4.70 4.66 4.18 (multiple peaks)	3.41	2.91 2.64 2.50 2.34 2.00	1.88 1.74 (multiple peaks)
Methanol extract	7.4 7.85 8.74			4.74 4.68 (double peak)	3.91 3.80 3.79 (multiple peaks)		1.89 1.31 1.29

polyphenols. The NMR results also showed that some of these materials still remained in the membranes even after the membranes were cleaned, and that it is these materials that cause irreversible fouling of the membrane.

4.2. Characterisation of juice samples

An understanding of the physico chemical nature of cane sugar juice as well as membranes is necessary if answers for minimising membrane fouling during juice treatment are to be found. The EDAX spectrum of the juice samples identified Si, C, O, and S as the main elements. Low levels of Al, Ca, K and Cu were also identified. In addition, the feed samples contain trace amounts of Zn and Fe. The feed sample showed a predominant Si background spectrum, and a higher Si to C peak ratio than the permeate and retentate juices. The spectrum of the retentate indicated a significant proportion of carbon containing species.

4.2.1. Shear behaviour

While chemical and microscopic evaluations provide structural characterisation of individual particles

and aggregates, information on complementary particle particle and polymer particle interactions on the organisation of aggregates can be obtained by rheological measurements.

The rheological behaviour of the feed stream is an important parameter affecting membrane fouling rates and mechanisms through wall interactions and particle particle structures. Reducing the viscosity of the feed stream (i.e. high shear or increased temperature) decreases the fouling rates by breaking particle networks and structural bonds to overcome viscous drag effects [20].

Fig. 6 shows the viscosity versus shear rate behaviour of the feed, retentate and permeate over a large shear rate range. The solutions appear non Newtonian (pseudo-plastic) and show shear thinning (i.e. decrease in viscosity with increasing shear rate) behaviour at intermediate shear rates ($1\text{--}10\text{ s}^{-1}$). At higher shear rates ($10\text{--}100\text{ s}^{-1}$) the viscosity is Newtonian. Evidence of shear thickening at $>100\text{ s}^{-1}$ (dilatancy) could be due to non laminar flow. More pronounced shear thickening is observed for the feed sample.

Viscosity values at low shear rates ($<1\text{ s}^{-1}$) relate to the behaviour under gravity and the level of network structure. Based on this, the feed sample showed a

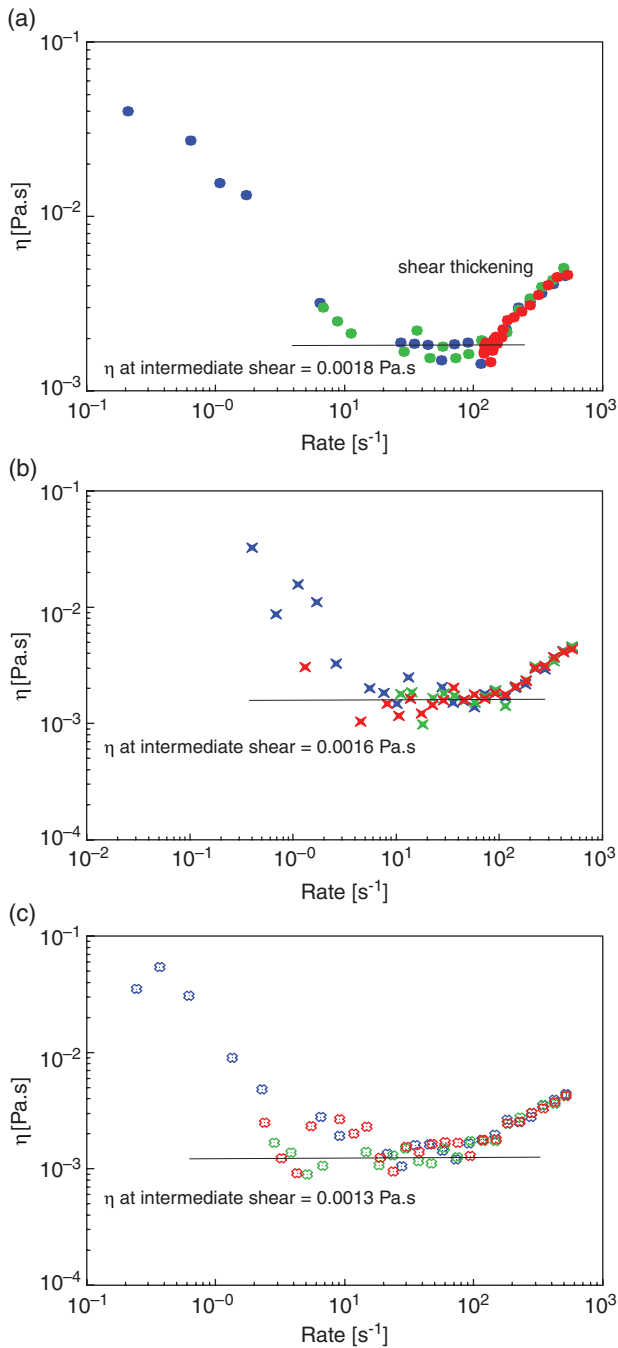


Fig. 6. Viscosity versus shear rate behaviour of (a) feed, (b) retentate and (c) permeate.

slightly increased level of network structuring and greater apparent viscosities than the permeate and retentate samples.

4.2.2. Dynamic rheology

The viscoelasticity of juice samples is likely to be dependent on the particle particle interactions and the

influence of polymers (i.e. polysaccharides) in solution. Weakly structured systems will respond to an applied stress or strain. Particular emphasis is given to the relationship between the storage modulus G' and the inter particle interactions.

Non-destructive dynamic stress sweep measurements may be obtained if the applied stresses or strains are within the linear viscoelastic region of a material. Fluids are relatively sensitive to structure breakdown and therefore have short linear viscoelastic regions. This is evident in Fig. 7 which shows the viscoelastic response of the juice samples to an applied stress <0.5 Pa. The linear region is defined as a stable G' output, which is independent of stress amplitude, i.e. $<2 \times 10^{-3}$ Pa in this case. At higher stresses, the structure of the material begins to break down and there is a rapid decline in the G' response. The feed sample appears considerably more structured than the retentate and permeate samples, i.e., higher G' values and longer linear viscoelastic region prior to structure breakdown.

4.2.3. Electroacoustics–zeta potential

The zeta potential (overall charge) values for the particles in the juice samples were determined by the Acoustosizer and the results are given in Table 5. The results show that the particles in the feed and those in the retentate have a lower net charge than the permeate particles, suggesting a greater tendency for the particles in the feed and those of the retentate to form aggregates. The implication of this is that the feed and the retentate will have a greater propensity to foul membranes, as would be expected.

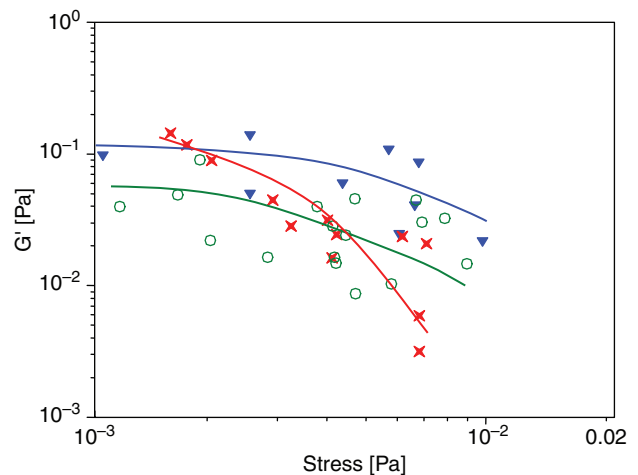


Fig. 7. Dynamic stress sweep of juice solutions where \blacktriangledown is for the feed; \times is for the retentate and \circ is for the permeate.

Table 5
Zeta potential measurements of juices.

Solution	pH	Zeta potential (mV)
Feed	7.15	10.0
Permeate	6.86	14.9
Retentate	6.97	8.8

4.2.4. Particle size distribution

Table 6 gives the particle size distribution data of the cane juice samples measured by laser diffraction after 1 min of mixing in the sample characterisation cell, without any sonication or dispersant addition. The measured particles do not represent the primary particles since they would have coagulated during storage because the juices were stored frozen to prevent deterioration. This in part explains the large particle sizes observed for the membrane treated cane juice samples. If coagulation of the particles did not take place, then the size of the particles in the permeate, assuming low aspect ratio, would be less than 0.1 μm which is the size of the membrane pores.

As the samples were stored under the same conditions, the results of Table 6 indicate distinct particle size differences between samples, with the permeate containing the finest size fractions.

The average size of the particles in the feed and retentate ought to be in the range 0.1–1.0 μm and that of the permeate should be <0.1 μm , since the pore size of the pre-filter is 1.0 μm and that of the ceramic membrane is 0.1 μm . The inference drawn from Table 6, neglecting coagulation of the particles during storage of the juices prior to analysis, indicates that the shape of some of the particles is such that the length is far greater than the width (i.e., high aspect ratio), resulting in large sizes being recorded by the Malvern instrument. Because the width of the particles is small, some may pass through

Table 6
Particle size distribution* of cane juice samples.

Sample	D (v, 0.1) (μm)	D (v, 0.5) (μm)	D (v, 0.9) (μm)	D [3,2] (μm)	D [4,3] (μm)
Feed	48.0	182.4	402.6	95.8	206.2
Permeate	31.3	75.1	153.2	58.2	86.6
Retentate	26.8	87.3	207.2	54.6	106.6

*D(v, 0.1) = 10% of the particle volume is less than or equal to that size; D(v, 0.5) = 50% of the particle volume is less than or equal to that size; D(v, 0.9) = 90% of the particle volume is less than or equal to that size; D[3,2] = the size of the particles weighted by surface area; D[4,3] = the size of the particles weighted by volume.

the pores of the ceramic membrane or block the pores of the membranes.

The particle size of the cane juice feed samples as a function of mixing time was also determined. A decrease in particle size was observed for the D(v, 0.5) data as shown in Fig. 8. This decrease is due to the breakdown of aggregates with increased conditioning and dissolution of some of the fine particles. The size reduction is most pronounced in the feed sample. This has implications in membrane fouling since extended conditioning (i.e., mixing) may be used to control and reduce the amount and number particles which will foul the membrane filters.

4.2.5. Summary

The studies on the interaction between juice constituents suggest that network structures are formed and that the feed is more structured than the permeate or retentate. Under high stresses, this structure begins to break down (Fig. 7 and Fig. 8). The Zeta potential values suggest that polymer-particle and particle-particle interactions will be occurring during membrane filtration (Table 5).

4.3. Fouling mechanism

The results have shown that organic materials (polysaccharides, proteins, lipids, polyphenols) with molecular weight >400 Da foul the membrane surface. Also, inorganic particles (including possibly calcium phosphate salt) from the feed get deposited on the membrane surface. These results indicate that particulate fouling is the main mechanism that occurs when cane juice is processed with tubular ceramic membranes. As the materials present in both the fouled and clean membranes are not dissimilar, the first step in the fouling mechanism would be a reversible process which would later be transformed into irreversible one as result of association between the components. The rheological and zeta potential information obtained from the juice suggests that the juice constituents are willing to form network structures and it is probable that this occurs on the membrane surface. This is not unreasonable since the SEM and in particular the XPS data show some degree of association between the polymers and the particles. This is confirmed from the DRIFT data which shows strong hydrogen bonding between the components.

5. Conclusion

A comprehensive assessment of the nature of the foulants deposited on a range of ceramic membranes

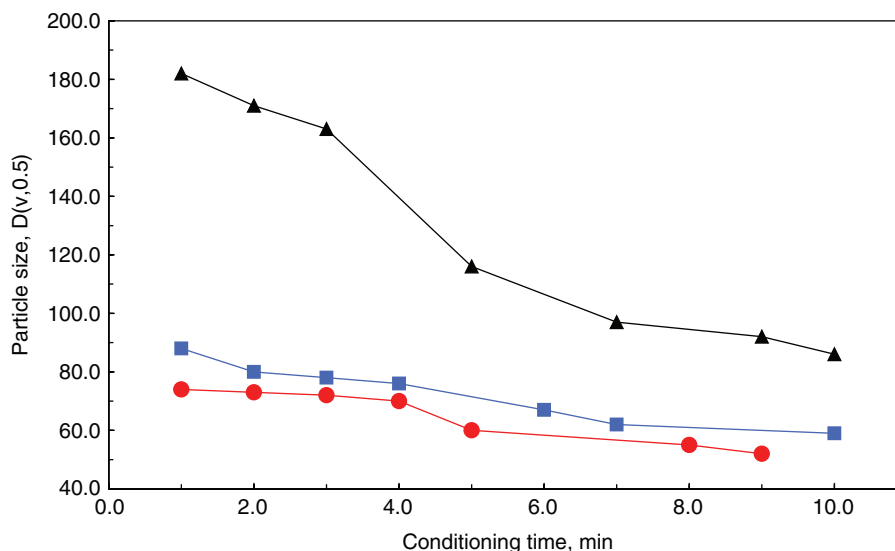


Fig. 8. Particle size data as a function of conditioning time where ▲ is for feed, ■ is for retentate and ● is for permeate.

in processing clarified juice has been undertaken. All the membranes, except the one with a pore size of 0.45 μm , generally gave reproducible results through the trials, were easy to clean and could handle operation at high VCFs.

Polysaccharides, lipids and polyphenols, as well as colloidal particles cause fouling of membranes. To combat irreversible fouling of the membranes, treatment options that result in the removal of particles having a size range of 0.2–0.5 μm and in addition remove polymeric materials, need to be identified. Disc stack centrifuges operating at a centrifugal force of 4,500–12,000 G are capable of removing these impurities in clarified juice. However, the capital and maintenance cost of these devices make them prohibitive for use in a raw sugar factory.

Based on the influence of polymers on particles and particle-particle interactions and the particle size and dynamic rheology results, another option that can be used to mitigate fouling of membranes is to condition (i.e., mix or agitate) clarified juice prior to membrane filtration. This is to fragment juice particles and break up the network structure formed between the polymers and particles [20] and assumed that the aggregates and structures do not reform after the conditioning step. However, this may be counterproductive as the membrane with the largest pores had the worst fouling, and so would presumably trap larger colloidal particles.

Use of a surfactant (e.g., maleate ester) as an additive prior to membrane filtration should assist to prevent the aggregation of polymers and particles and their adhesion to surfaces, and hence reduce the amount of foulants trapped in the membrane pores.

References

- [1] R.J. Steindl, Membrane filtration technology in the cane sugar industry, *Proc. Int. Soc. Sugar Cane Technol.*, 24 (2001) 3–14.
- [2] R.J. Steindl and C.D. Doyle, Applications and benefits of membrane filtration for the Australian sugar industry, *Proc. Aust. Soc. Sugar Cane Technol.*, 21 (1999) 406–411.
- [3] R.F. Madsen, Application of ultrafiltration and reverse osmosis to cane juice, *Int. Sugar. J.*, 75 (1973) 163–167.
- [4] A.C. Eringis, and B. Eaton, Ultrafiltration of clarified cane juice, *Proc. Sugar Processing Res. Conf. (SPRI)*, (2000) 286–291.
- [5] S. Cartier, M.A. Theoleyre, and M. Decloux, Treatment of affination syrup by micro/ultrafiltration: impact on crystallisation process, *Proc. Sugar Industry Technol.*, 56 (1997) 133–145.
- [6] R.J. Kwok, Ultrafiltration/softening of clarified juice – the door to direct refining and molasses desugarisation in the cane sugar industry, *Proc. S. Afr. Sug. Technol. Ass.*, 70 (1996) 166–170.
- [7] J.P. Monclin, and S.C. Willett, The ‘A.B.C. Process’ for the direct production of refined sugar from cane mixed juice, *Proc. S.P.R.I. Workshop on Separation Processes in the Sugar Industry*, (1996) 16–28.
- [8] M. Saska, J.C. McArdle, and A.C. Eringis, Filtration of clarified juice using spiral polymeric membrane configuration. *Proc. Int. Soc. Sugar Cane Technol.*, 23 (1999) 17–25.
- [9] W.L. Fechter, S.M. Kitching, M. Rajh, R.H. Reimann, F.E. Ahmed, C.R.C. Jensen, P.M. Schorn, and D.C. Walthew, Direct production of white sugar and whistrap molasses by applying membrane and ion exchange technology in a cane sugar mill. *Proc. Int. Soc. Sugar Cane Technol.*, 24 (2001) 100–107.
- [10] A.M. Ghosh, and M. Balakrishnan, Pilot demonstration of sugarcane juice ultrafiltration in an Indian sugar factory. *J. Food Eng.*, 58 (2003) 143–150.
- [11] T. Martoyo, M. Hino, H. Nagase, and A. Bachtiar, Pilot test on ultrafiltration of cane raw juice at the Indonesian plantation white Kedawoeng sugar factory. *Zuckerindustrie*, 125 (10) (2000) 787–792.

- [12] S.J. Clark, (2000). *Personal communication*.
- [13] R.J. Kwok, X. Lancrenon, and M.A. Theoleyre, Process manufacturing crystal sugar from aqueous sugar juice such as cane juice or sugar beet juice, US Patent no: 5, 554,227, 1996.
- [14] W.L. Fechter, S.M. Kitching, Reimann, R. H., Ahmed, F. E., Jensen, C. R. C., Schorn, P. M. and Walthew, D. C., (2001). Direct production of white sugar and whitestrap molasses by applying membrane and ion-exchange technology in a cane sugar mill. *Proc. Int. Soc. Sugar Cane Technol.*, 24: 100-107.
- [15] J.R. Vercellotti, M.A. Clarke, M.A. Godshall, R.S. Blanco, W.S. Patout, and R.A. Florence, Chemistry of membrane separation processes in sugar industry applications. *Zuckerindustrie*, 123(9) (1998) 736–745.
- [16] J.R. Vercellotti, M.A. Clarke, and M.A. Godshall, Sugarcane components that affect efficiency of membrane filtration: identification and removal. *Proc. Int. Soc. Sugar Cane Technol.*, 23 (1999) 26–41.
- [17] C.M. Fellows, and W.O.S. Doherty, Insights into bridging flocculation. *Macromolecular Symposia*, 231 (2006) 1–10.
- [18] S.P. Beaudoir, C.S. Grant, and R.G. Carbonell, Removal of organic films from solid surfaces using aqueous solution of non-ionic surfactants. *Ind. Eng. Chem. Res.*, 34 (1995) 3307–3317.
- [19] M. Cheryan, *Ultrafiltration Handbook*. Technomic Publishing Company, Inc., Pennsylvania, 1986.
- [20] J. Bruijn and R. Borquez, Analysis of the fouling mechanisms during cross-flow ultrafiltration of apple juice. *LWT – Food Sci. Tech.*, 39 (2006) 861–871.